ELKOMIKA: Jurnal Teknik Energi Elektrik, Teknik Telekomunikasi, & Teknik Elektronika

ISSN(p): 2338-8323 | ISSN(e): 2459-9638 | Vol. 12 | No. 2 | Halaman 367 - 377
DOI : http://dx.doi.org/10.26760/elkomika.v12i2.367 April 2024

4.5 kW High Frequency Transformer Design for Dual Active Bridge (DAB)

NAUFAL HILMI FAUZAN, EKA FIRMANSYAH, FELIX AUSTIN CAHYADEWA

Universitas Gadjah Mada, Indonesia
Email: naufalhilmifauzan@ugm.ac.id

Received 19 Oktober 2023 **|** *Revised* 3 Desember 2023 **|** *Accepted* 16 Desember 2023

ABSTRAK

Indonesia bertujuan untuk beralih dari bahan bakar fosil ke sumber energi terbarukan, dengan target integrasi sebesar 23% pada tahun 2025 dan 31% pada tahun 2050. Transisi ini menghadapi tantangan akibat sifat terputus-putus dari sumber energi terbarukan yang memengaruhi kualitas listrik. Solid State Transformer (SST) muncul sebagai solusi. Dalam penelitian ini, sebuah trafo frekuensi tinggi dirancang untuk konverter Dual Active Bridge (DAB), dengan leakage inductance menjadi parameter penting. Berdasarkan perhitungan yang dilakukan, menunjukkan kebutuhan leakage inductance adalah sebesar 277 µH untuk DAB. Untuk memenuhi kebutuhan daya dan nilai leakage inductance tersebut, trafo dengan inti EE48020, 87 lilitan non-seksional, dan ketebalan isolasi 8,4 mm dapat dikembangkan. Hasil simulasi mengkonfirmasi nilai leakage inductance yang dihasilkan sebesar 268,95 µH.

***Kata kunci**: tranformator frekuensi tinggi, dual active bridge, solid state transformer, kebocoran induktansi, geometri inti*

ABSTRACT

Indonesia aims to shift from fossil fuels to renewable energy sources, targeting 23% integration by 2025 and 31% by 2050. This transition faces challenges due to the intermittent nature of renewable sources, impacting power quality. Solid-state transformers (SST) emerge as a solution. In this study, a high-frequency transformer (HFT) is designed for the dual active bridge (DAB), with leakage inductance being a crucial parameter. Calculations indicate a 277 µH requirement for the DAB. To meet power needs and leakage inductance values, an HFT with an EE48020 core, 87 non-sectional turns, and 8.4 mm insulation thickness is developed. Simulation results confirm a leakage inductance of 268.95 µH for the HFT.

***Keywords**: high frequency transformer, dual active bridge, solid state transformer, leakage inductance, core geometry*

1. INTRODUCTION

Indonesia has a target to increase renewable energy sources and begin transitioning from fossil fuels. The target for the renewable energy mix in 2025 is 23% and in 2050 is 31% **(Winarno et al., 2017)**. Additionally, the Indonesian Government issued Presidential Regulation No. 55 of 2019 to accelerate the electric vehicle program based on battery-powered vehicles for road transportation. This serves as the legal framework for the development of electric vehicles in Indonesia **(Maghfiroh et al., 2021)**. The targets for renewable energy development and electric vehicles are solutions to environmental issues **(Saber & Vebatagamoorthy, 2011)**. However, they pose challenges to the power system, particularly concerning power quality **(Ayadi et al., 2020)**. Renewable energy sources cause voltage and frequency deviations due to intermittent. Conventional transformers have limitations such as large size and weight, low efficiency at light loads, and passive behavior during transient conditions. These issues can be addressed by smart transformers, also known as solid-state transformers (SST) **(Parihar et al., 2022) (Zhao et al., 2020)**. The implementation of SST in the electric power distribution system represents a future solution, as shown in Figure 1 **(Ruiz et al., 2020)**.

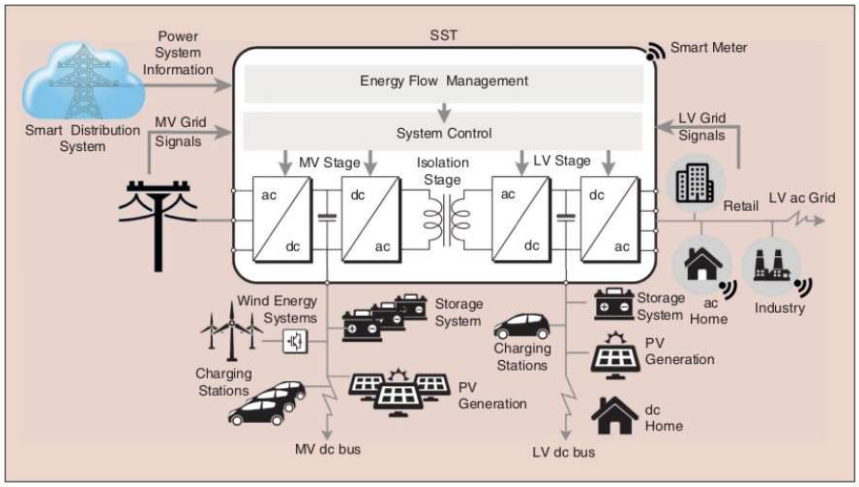

Figure 1. Future Power Distribution System

Based on Figure 1, SST is a power transformer consisting of power electronics converters and medium/high-frequency transformers. The high-frequency transformer (HFT) operates at high frequencies, ranging from kilohertz to megahertz, whereas conventional transformers typically operate at the frequency of the electrical grid (50 or 60 Hz) **(Gautam et al., 2018) (She et al., 2013)**. The high operating frequency allows the transformer to have a smaller size and lighter weight compared to conventional transformers with the same output power **(She et al., 2013)**. This makes HFT a suitable choice for applications where compact size and lightweight are essential, such as in portable electronic devices and distributed power systems. Furthermore, the implementation of HFT can also provide current and voltage regulation, current limiting, and energy storage management **(Tariq et al., 2020)**. In the solid-state transformer, the high-frequency transformer serves as galvanic isolation and supplies a leakage inductance value for dual active bridge (DAB) **(Rahrovi et al., 2021) (Zhang et al., 2022)**. DAB is a commonly used converter topology in high-frequency transformer applications due to its ability to provide high power density and efficiency. The schematic of the DAB converter topology is shown in Figure 2 **(Dey et al., 2022)**.

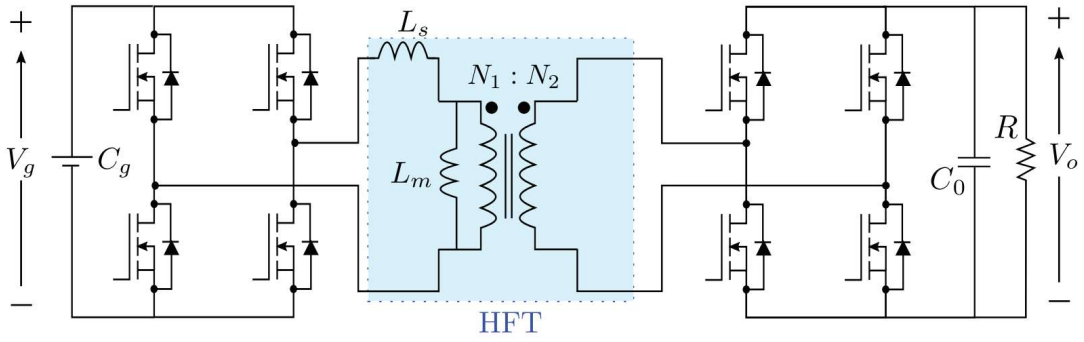

Figure 2. Schematic of Dual Active Bridge (DAB) Converter

In the DAB converter, adjustments to the leakage inductance value of the transformer are necessary to stable power conversion and reduce switching losses that can impact its operational efficiency **(Hoang & Wang, 2012)**. The value of leakage inductance can be tailored through designing an appropriate transformer layout, particularly in selecting winding configurations and the insulation gap between the two windings **(Ouyang et al., 2009)**. Commonly used winding configurations in transformer design include conventional, sectional, and interleave types **(McLyman, 2004) (Zhang et al., 2022)**.

High-frequency transformers need to be developed and further researched to ensure their suitability and benefit for the progress of Indonesia. This is done to support the performance of Solid-State Transformers (SST) in Indonesia. Hence, the goal of this research is to design and simulate a high frequency transformer suitable for DAB, while considering the leakage inductance value.

2. RESEARCH METHOD

This research was conducted through experiments in the form of high-frequency transformer simulations using Ansys PEmag and Ansys Electronics Desktop. The design of the transformer began with determining initial specifications, including operating power (P), frequency (f), voltage (V), maximum duty cycle (D_{max}), window utilization (K_u), operating flux density (B_{ac}), waveform factor (K_f), voltage regulation (α), and efficiency (η). These specifications were used for calculating supporting parameters, especially in the selection of the transformer core and the number of windings along with their strands. The determination of the transformer core was based on the core geometry method, involving calculations and comparisons of core geometry requirements against available core sizes **(Heathcote, 2007)**.

The calculations commenced with the computation of the wire diameter (D_{awg}). The calculated wire diameter (D_{awg}) served as a reference for choosing the wire diameter from available options in the datasheet, with the criterion that $D_{wire} > D_{awg}$ must be satisfied. The obtained diameter then became a parameter for calculating the apparent power (P_t) and electrical condition (K_e). The P_t and K_e data were needed for the calculation of core geometry (K_g), which was used to guide core selection by referring to the existing datasheet. The equation that represents the determination of core geometry can defined in Equation 1:

$$K_g = \frac{P_t \times 1.35}{2 \times K_e \times \alpha} \quad (cm^5) \tag{1}$$

The core can be considered usable when the calculated core geometry value exceeds the transformer's core geometry value (K_g) in the datasheet. The core geometry value provided by the transformer's core can be determined and defined in Equation 2:

$$K_{g,core} = \frac{{A_c}^2 \times W_a}{MLT} \quad (cm^5) \tag{2}$$

Where A_c represents the cross-sectional area and MLT represents the mean length turn. Once the core geometry value meets the criteria, the number of windings (N) and their strands (S_n) can be determined. The total number of windings along with their strands are used in calculating the window area (W_a) of the transformer. The calculated W_a value is then compared to the available $W_{a,core}$ value in the datasheet. If the value of $W_{a,core}$ is greater than the calculated value, it can be concluded that the utilized transformer core is suitable and can be used.

After obtaining all parameters, the next step involves determining the leakage inductance capacity in the DAB converter. To calculate the value of leakage inductance needed by DAB, Equation 3 can be used **(Rahrovi et al., 2021) (Texas Instrument, 2019)**.

$$P = \frac{n \times V_{in} \times V_{out}}{2\pi \times f \times L_p} \, \varphi\left(1 - \frac{\varphi}{\pi}\right) \quad (H) \tag{3}$$

Where P is input power, n is winding ratio, V_{in} is input voltage, V_{out} is output voltage, f is frequency, L_p is the leakage inductance, and φ is phase shift between the primary and secondary square-wave voltage. The maximum power transfer at a specific switching frequency, leakage inductance, and input-output voltage happens when $\varphi = \frac{\pi}{2}$ and the Equation 4 will be obtained.

$$L_p = \frac{n \times V_{in} \times V_{out}}{8 \times f \times P} \quad (H) \tag{4}$$

Based on this leakage inductance capacity, the insulation thickness between the two windings can be determined. To calculate the value of leakage inductance generated in the transformer, Equation 5 can be used .

$$L_p = \frac{4 \times \pi \times MLT \times Np^2}{a} \cdot \left(c + \frac{\Sigma b}{3}\right) \cdot (10^{-9}) \quad (H) \tag{5}$$

Where N_p is the primary turn, a is the winding length, b is the winding build, and c is the insulation thickness. Subsequently, the determination of winding configuration can be carried out, and in this research, a conventional winding configuration type will be used. Following this, the design and simulation process is carried out using the Ansys Electronics Desktop software. This simulation process produces a complete HFT design in accordance with the specified specifications, including flux distribution, induced voltage, losses, and leakage inductance.

3. DESIGN AND RESULT

3.1. Core and Winding Considerations

Based on the method outlined in the previous chapter, it is known that the first step carried out is the determination of specifications for this research. The specifications used in this research are presented in Table 1.

Table 1. Transformer Specifications

Parameters	Value
Power	4.5 kW
Input – output voltage	1 kV – 1 kV
Frequency	100 kHz
Operating flux density	0.1 T
Waveform factor	4
Maximum duty cycle	0.5
Window utilization	0.2
Regulation	0.5
Efficiency	90%

After the specifications have been established, the next step involves conducting calcuations to determine the transformer core to be used. The results of the transformer core calculation are presented in Table 2.

Table 2. The Results of the Transformer Calculation

Parameters	Value
Bare wire area	0.138 mm^2
Apparent power	9.5 kW
Electrical condition	23,200
Core geometry	0.553 cm^5
Area product	23.75 cm^4

Based on the calculation results in Table 2, the bare wire area (A_ω) is used to determine the type of cable to be used. With this bare wire area, an AWG#26 cable with a bare wire area of *0.13 mm^2* will be used **(Calmont, 2022)**. According to the core geometry calculation results in Table 2, a *Magnetics* EE48020 transformer core will be utilized, with a cross-sectional area of *2.88 cm^2*, winding area of *10.97 cm^2*, and core geometry of *5.72 cm^5* **(Magnetics, 2022)**. Along with determining the core size, the number of turns and strands have also been determined, totaling 87 turns with 6 strands. According to the *American Wire Gauge* (AWG) chart published by Calmont **(Calmont, 2022)**, there is no availability of cable with 6 strands of AWG#26. Therefore, in this research, a cable that closely approximates it will be used, which is the 7 strands of AWG#26 with a diameter of *1.21 mm*. After that, the calculated winding area (W_a) needed for this research is *8.7 cm^2*. It can be concluded that the EE48020 transformer core is suitable for this research due to the provided winding area of the core being suifficient for the required winding area. Besides being determined through the core geometry method, core selection can also be made by referring to the Power Handling Chart and Area Product Distribution Chart provided by *Magnetics* as shown in Figure 3 and Figure 4 **(Magnetics, 2022)**.

Typical Power Handling Chart

Power in Watts				Pot, RS, DS	E Cores	RM, PQ, EP	UU, UI, UR	ETD, EER, EC	EFD, Planar	Toroid
20 kHz	50 kHz	100 kHz	250 kHz							
2000	3000	4500	8750		46527 EE 47133 EE 48020 EE					46325 TC 46326 TC 47313 TC

Figure 3. Power Handling Chart by *Magnetics*

Area Product Distribution (WaAc) Chart

WaAc (cm^4)	RS, DS, HS	E	EC, EER, EFD, ETD	EP, RM	ER	Planar	Pot	PQ	TC	U, UR
34		48020 EE							46325 TC 46326 TC	

Figure 4. Area Product Distribution Chart by *Magnetics*

Based on Figure 3, it is evident that for a transformer with a frequency specification of 100 kHz and a power of 4500 W, there are several core type options available, and one of these is the EE48020. This is further supported by the area product of EE48020 core as shown in Figure 4, where the core can provide the required area product for this research. In this research, the transformer design also utilized a bobbin provided by *Magnetics*, namely 00B8020B1.

Based on Equation 3, the required value of leakage inductance for the DAB converter can be calculated, which amounts to $277.78\,\mu H$. Using the calculated leakage inductance value, the required insulation thickness for this research can also be determined using Equation 5.

3.2. Calculation and Simulation Analysis

In this section, the calculated leakage inductance values will be compared and verified against simulation result. The simulation was conducted using Ansys Electronics Desktop to determine the leakage inductance value of the constructed transformer. The transformer design created by Ansys can be shown in Figure 5.

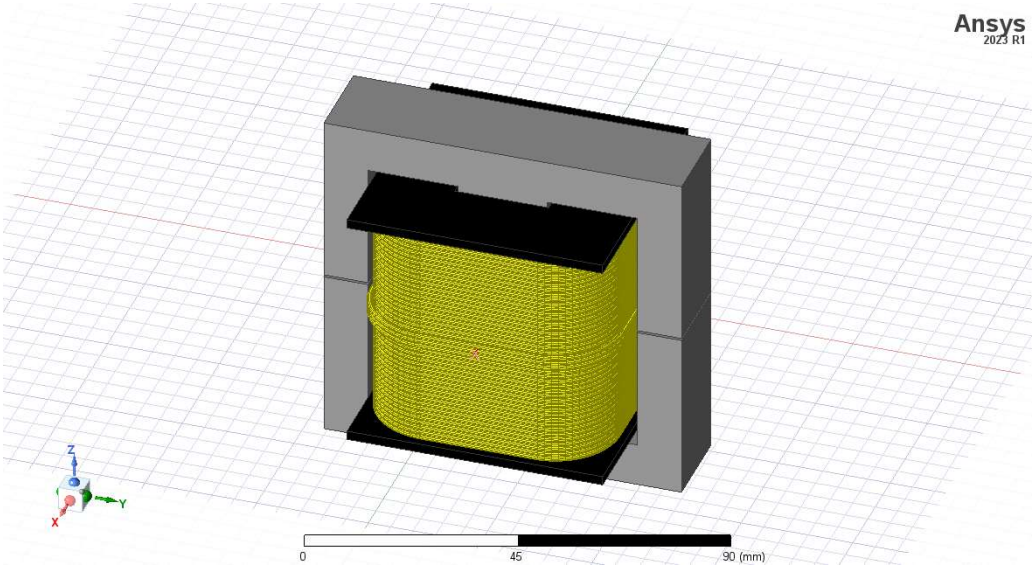

Figure 5. High frequency transformer design

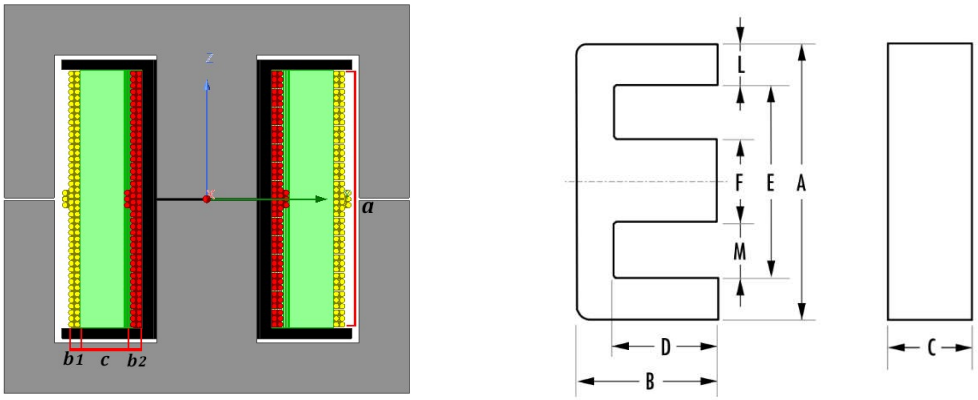

(a) **(b)**

Figure 6. Dimensional Notation Used. (a) Width and Height Winding Build, (b) Core Dimensions

Table 3. The Dimensions Used in This Research

Dimensions (mm)										
A	B	C	D	E	F	L	M	a	$b1$	$b2$
80	38.1	19.8	28.2	59.1	19.8	11.25	19.45	50.82	3.63	3.63

In the simulation, variations in the insulation thickness will be performed. Based on **(Yang et al., 2022)**, it is known that the simulation result consistently produces smaller leakage inductance values compared to the calculated one, and the insulation thickness separating the two windings will affect the leakage inductance value.

In this research, it is known that the maximum value of leakage inductance required by DAB is $277\ \mu H$. By modifying Equation 5 and setting the leakage inductance to $277\ \mu H$, it was determined that the required insulation thickness is $6.9\ mm$. After conducting simulations with an insulation thickness of $6.9\ mm$, the resulting leakage inductance value for the transformer was $228.55\ \mu H$. This value is significantly below the expected leakage inductance value.

Using the previously obtained data, extrapolation was performed to determine the insulation thickness that would result in a leakage inductance value close to $277\ \mu H$. Based on the extrapolation result, it was determined that the required insulation thickness is approximately $8.4\ mm$. With this $8.4\ mm$ insulation thickness and the use of Equation 5, the calculated leakage inductance value is $322.39\ \mu H$. Meanwhile, simulation result with an $8.4\ mm$ insulation thickness yielded a leakage inductance value of $268.95\ \mu H$. This value is still below the desired leakage inductance.

By optimizing the window area utilization, this research transformer can achieve a maximum insulation of $8.6\ mm$. The use of this insulation results in a leakage inductance calculation of $328.35\ \mu H$, as referred to Equation 5. Meanwhile, the simulation results for leakage inductance with $8.6\ mm$ insulation are $274.41\ \mu H$. The comparison graph of leakage inductance values and the insulation thickness used in this research can be shown in Figure 7.

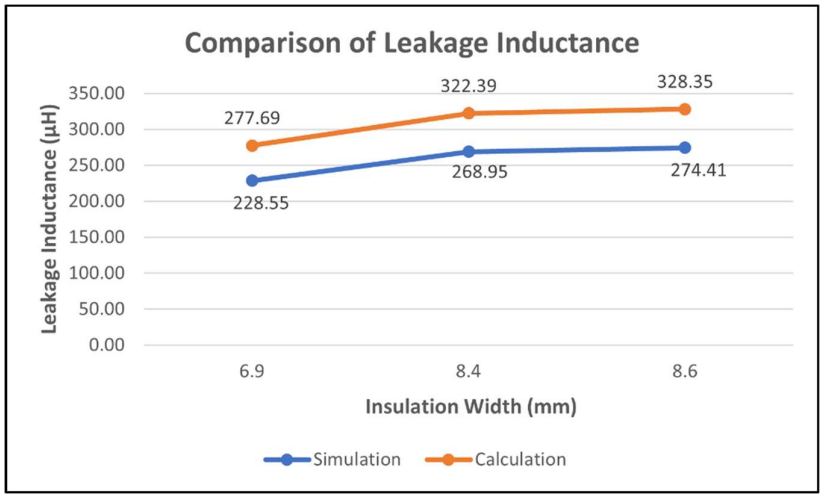

Figure 7. Comparison between Leakage Inductance and Insulation Thickness Used

Based on Figure 7, the simulation result consistently yields lower values of leakage inductance compared to calculations results. The result obtained in this research are aligned with the findings presented in **(Yang et al., 2022)**. One of the reasons for the difference between calculation and simulation result is that the Mean Length Turn (MLT) value derived from the core, with an estimated bobbin representing 20% of the core's winding area, as specified in **(Elrajoubi & Ang, 2019) (Hoang & Wang, 2012)**. Meanwhile, in simulations conducted using Ansys software, the MLT value used is the actual MLT value of the winding of the winding used.

4. CONCLUSION

For a DAB operating at 100 kHz and 4.5 kW power, a leakage inductance of $277\ \mu H$ is required. This leakage inductance value is necessary to enable soft switching and reducing losses. In this research, the high frequency transformer was designed using an EE48020 core from *Magnetics*, a bobbin with the type 00B8020B1, #AWG26 wire with 7 strands inside, and 87 turns on both the primary and secondary sides. Based on the research findings, to achieve a leakage inductance value close to $277\ \mu H$, insulation with a thickness of $8.4\ mm$ was chosen because it can yield a leakage inductance value of $268.95\ \mu H$. The selection of this insulation is based on the DAB's leakage inductance requirements. Additionally, the choice of $8.4\ mm$ thickness was chosen because it doesn't completely fill the transformer's window area, allowing for the addition of insulation on the outer winding side as necessary.

NOTATION

Notation

f : Frequency
P : Input power
α : Voltage regulation
P_t : Apparent power
K_e : Electrical condition
A_C : Cross-sectional area
W_a : Window area

MLT: Mean length turn
n : Winding ratio
V_{in} : Input voltage
V_{out} : Output voltage
φ : Phase shift between the primary and secondary square-wave voltage
N_P : Number of primary turns
a : Winding length
b : Winding build
c : Insulation thickness

ACKNOWLEDGEMENT

The authors thank Young Lecturer Research Grant Universitas Gadjah Mada Number 5985/UN1.P.II/Dit-Lit/PT.01.03/2023 for supporting this research activity, colleagues in the Department of Electrical and Information Engineering, Universitas Gadjah Mada and High Voltage Engineering Laboratory assistant who have fully supported, and to the entire team that has assisted this research.

REFERENCES

Ayadi, F., Colak, I., Garip, I., & Bulbul, H. I. (2020). Impacts of Renewable Energy Resources in Smart Grid. *2020 8th International Conference on Smart Grid (IcSmartGrid)*, (pp. 183–188). https://doi.org/10.1109/icSmartGrid49881.2020.9144695

Calmont. (2022). *Solid and Stranded Conductor AWG Chart*. https://www.calmont.com/wp-content/uploads/calmont-eng-wire-gauge.pdf

Dey, S., Chakraborty, S. S., Singh, S., & Hatua, K. (2022). Design of High Frequency Transformer for a Dual Active Bridge (DAB) Converter. *2022 IEEE Global Conference on Computing, Power and Communication Technologies (GlobConPT)*, (pp. 1–6). https://doi.org/10.1109/GlobConPT57482.2022.9938249

Elrajoubi, A. M., & Ang, S. S. (2019). High-Frequency Transformer Review and Design for Low-Power Solid-State Transformer Topology. *2019 IEEE Texas Power and Energy Conference (TPEC)*, (pp. 1–6). https://doi.org/10.1109/TPEC.2019.8662131

Gautam, S. P., Kedia, S., Bahirat, H. J., & Shukla, A. (2018). Design Considerations for Medium Frequency High Power Transformer. *Proceedings of 2018 IEEE International Conference on Power Electronics, Drives and Energy Systems, PEDES 2018*, (pp. 2370–2375). https://doi.org/10.1109/PEDES.2018.8707697

Heathcote, M. J. (2007). *J & P Transformer Book, Thirteenth Edition*. https://doi.org/https://doi.org/10.1016/B978-0-7506-8164-3.X5000-5

Hoang, K. D., & Wang, J. (2012). Design optimization of high frequency transformer for dual active bridge DC-DC converter. *2012 XXth International Conference on Electrical Machines*, (pp. 2311–2317). https://doi.org/10.1109/ICElMach.2012.6350205

Maghfiroh, M. F. N., Pandyaswargo, A. H., & Onoda, H. (2021). Current readiness status of electric vehicles in indonesia: Multistakeholder perceptions. *Sustainability (Switzerland)*, *13*(23), 1–25. https://doi.org/10.3390/su132313177

Magnetics. (2022). *Magnetics Ferrite Cores*. https://www.mag-inc.com/Media/Magnetics/File-Library/Product%20Literature/Ferrite%20Literature/Magnetics-2022-Ferrite-Catalog.pdf?ext=.pdf

McLyman, C. W. T. (2004). *Transformer and inductor design handbook*. Marcel Dekker.

Ouyang, Z., Thomsen, O. C., & Andersen, M. A. E. (2009). The analysis and comparison of leakage inductance in different winding arrangements for planar transformer. *2009 International Conference on Power Electronics and Drive Systems (PEDS)*, (pp. 1143–1148). https://doi.org/10.1109/PEDS.2009.5385844

Parihar, K. S., Khan, W., Dar, J. A., & Pathak, M. K. (2022). A Hybrid modulation scheme for AC-AC Dual Active Bridge-based Solid-State Transformer. *2022 IEEE International Conference on Power Electronics, Drives and Energy Systems (PEDES)*, (pp. 1–6). https://doi.org/10.1109/PEDES56012.2022.10080750

Rahrovi, B., Mehrjardi, R. T., & Ehsani, M. (2021). On the Analysis and Design of High-Frequency Transformers for Dual and Triple Active Bridge Converters in More Electric Aircraft. *2021 IEEE Texas Power and Energy Conference (TPEC)*, (pp. 1–6). https://doi.org/10.1109/TPEC51183.2021.9384990

Ruiz, F., Perez, M. A., Espinosa, J. R., Gajowik, T., Stynski, S., & Malinowski, M. (2020). Surveying Solid State Transformer Structures and Controls Providing Highly Efficient and Controllable Power Flow in Distribution Grids. *IEEE Industrial Electronics Magazine*, *14*, 56–70. https://doi.org/10.1109/MIE. 2019.2950436

Saber, A. Y., & Vebatagamoorthy, G. K. (2011). Plug in Vehicles and Renewable Energy Sources for Cost and Emission Reductions. *IEEE Transactions on Industrial Electronics*, *58*, 1229–1238. https://doi.org/10.1109/TIE.2010. 2047828

She, X., Huang, A. Q., & Burgos, R. (2013). Review of solid-state transformer technologies and their application in power distribution systems. *IEEE Journal of Emerging and Selected Topics in Power Electronics*, *1*(3), 186–198. https://doi.org/10.1109/JESTPE.2013.2277917

Tariq, M., Iqbal, M. T., Maswood, A. I., & Ullah Khan, M. S. (2020). Dual Transformer Based Dual Active Bridge for Solid State Transformer in Distribution System. *IECON 2020 The 46th Annual Conference of the IEEE Industrial Electronics Society*, (pp. 3666–3671). https://doi.org/10.1109/IECON43393.2020.9254781

Texas Instrument. (2019). *Bidirectional, Dual Active Bridge Reference Design for Level 3 Electric Vehicle Charging Stations*. www.ti.com

Winarno, O. T., Alwendra, Y., & Mujiyanto, S. (2017). Policies and strategies for renewable energy development in Indonesia. *2016 IEEE International Conference on Renewable Energy Research and Applications, ICRERA 2016*, (pp. 270–272). https://doi.org/10.1109/ICRERA.2016.7884550

Yang, Z., Tahir, M., Hu, S., Huang, Q., & Zhu, H. (2022). Transformer Leakage Inductance Calculation Method with Experimental Validation for CLLLC Converter Topology. *Energies*, *15*(18), 1–14. https://doi.org/10.3390/en15186801

Zhang, X., Xiao, F., Wang, R., Kang, W., & Yang, B. (2022). Modeling and Design of High-Power Enhanced Leakage-Inductance-Integrated Medium-Frequency Transformers for DAB Converters. *Energies*, *15*(4), 1–23. https://doi.org/10.3390/en15041361

Zhao, Y., Zhang, G., Liao, Z., Wan, L., Li, Y., & Yang, F. (2020). Optimal Design of Insulation Structure of HV-HF Transformer Based on High-Frequency Insulation Properties of Gas-Solid System. *2020 IEEE Electrical Insulation Conference (EIC)*, (pp. 482–485). https://doi.org/10.1109/EIC47619.2020.9158702